Synthesis and characterisation of control porosity resorcinol formaldehyde based carbon aerogels under different conditions

Abbas, Qaisar; Mirzaeian, Mojtaba; Swanson, Hannah

Published in:
Materials Science & Smart Materials (MSSM)

Published: 01/01/2018

Document Version
Publisher's PDF, also known as Version of record

SYNTHESIS AND CHARACTERISATION OF CONTROL POROSITY RESORCINOL FORMALDEHYDE BASED CARBON AEROGELS UNDER DIFFERENT CONDITIONS

Q. Abbas[1]*, M. Mirzaeian[2]* and H. Swanson[3]

1. School of Engineering and Computing, University of the West of Scotland, Paisley, UK; email: qaisar.abbas@uws.ac.uk email: mojtaba.mirzaeian@uws.ac.uk

ABSTRACT

Highly porous carbon aerogels are synthesised by sol-gel polymerisation of resorcinol (R) and formaldehyde (F) using sodium carbonate (C) as catalyst followed by carbonization under steady flow of argon (Ar). The effect of resorcinol / catalyst (R/C) ratio and carbonization temperature on the porous structure of resultant gels and carbons was investigated using nitrogen adsorption-desorption measurements at -196 ºC. By controlling the R/C ratio between 100 − 500 and carbonization temperature between 800 − 1000 ºC carbon aerogels with specific surface areas (SSA) ranging between 537 − 687 m^2g^{-1} and average pore size in the range of 1.80 − 4.62 nm can be produced. It has been shown that carbonization had significant effect on the porous structure of the resultant carbon aerogels, decreasing the pore size and increasing the microporosity of the carbon due to the shrinkage of the nanostructure and the formation of microporosity within the gel structure. Substantial change in micro structure of carbon aerogels was observed at carbonization temperature of 800 ºC which resulted in highest specific surface area and pore volume without any considerable change in average pore size. BET specific surface area and pore volume increased from 687 to 1775 m^2g^{-1} and 0.24 to 0.94 cm^3g^{-1} respectively whereas the pore size remained constant (around 2nm) after physical activation of the carbon aerogels using CO_2 as an activation agent.

Keywords: Carbon aerogels, Specific surface area, Carbonisation, Activation agent

1 INTRODUCTION

Carbon materials have been used in wide range of application such as adsorbent for gas separation, catalytic processing, water purification, environmental protection and electrode materials for various energy storage devices. Extensive research studies have been conducted in order to produce carbon materials with desired porous properties for their use in practical applications in particular area. However, for each specialised application tailoring of various parameters such, pore size, specific surface area and pore size distribution with ease of processability in a cost effective manner is still a challenge. Resorcinol- formaldehyde (RF) based organic / carbon aerogels first synthesised by Pakela et al[1-3] according to poly-condensation reaction mechanism which is analogous to the sol-gel synthesis of inorganic oxides[4].The increasing popularity of these aerogels is due to controllability of textural parameters such as surface area and pore size as a functional of different synthesis parameters e.g. type of organic precursor, drying and curing methods and carbonization / activation conditions. By controlling these synthesise parameters carbon aerogels with desired structural properties tailored for each application can be produced [5-7].

In present study, resorcinol- formaldehyde (RF) based organic / carbon aerogels with control porosity have been prepared and effect of various synthesis parameters including resorcinol/ catalyst ratio, carbonisation / activation temperature, CO2 flow rate on various porous parameters (average pore size, pore size distribution, specific surface area , pore volume and wettability have been assessed.

2 EXPERIMENTAL

2.1 Synthesis of R/F gels

Resorcinol (R) formaldehyde (F) aerogels were prepared by polycondensation reaction between resorcinol and formaldehyde according to the procedure explained elsewhere [5, 8].

2.2 Carbonization of R/F aerogels (RFC)

The dried RF aerogels were carbonized at different temperatures to investigate the effect of pyrolysis conditions on the porous structure of carbon aerogels the procedure explained elsewhere [9].

2.3 Activation of R/F aerogels (RFCA)

Carbon samples were activated by physical activation at different temperatures using CO_2 as activation agent the procedure explained elsewhere [10].

3 PHYSICAL CHARACTERIZATIONS

The porous structure of RF aerogels and carbon was characterized by a Tri-Star adsorption analyser (Micromeritics). The samples were evacuated in a vacuum oven at 80 ºC at 5 mbar for 24 h and then they were further purged in a nitrogen flow at elevated temperatures (80 ºC for gels samples and 300 ºC for carbons) in a Flowprep system (Micrometrics) prior to the adsorption/desorption measurements. BET method was used for surface area measurements, t-plot method was used for micropore analysis, and BJH method using adsorption branch of the isotherm was used to calculate pore size distribution. The total pore volume was determined from the adsorbed volume of nitrogen at saturation pressure (P/Po = 0.99) [11].

Contact angle measurements were carried out using a CAM 200 goniometer system manufactured by KSV Ltd based on video captured images and automatic image analysis using CAM software. 6M KOH was used as the probe liquid for the determination of contact angles.

Raman spectroscopy was carried out on an "In via Raman microscope (Renishaw, UK)" with 514.5 nm diode laser excitation in the range of 1000 cm^{-1} and 3000 cm^{-1} to evaluate the vibrational properties of the electro-active material.

4 RESULTS AND DISCUSSIONS

4.1 BET analysis of the samples

Figure 1 shows the N_2 adsorption-desorption isotherms of RF gels. All isotherms show a type IV isotherm with H2-type hysteresis loop which is the indicative of well-developed micro and messoporisity within the gel structure [12]. Samples with R/C ratio of 100, show a microporous structure with the absence of the hysteresis loop. For samples with R/C ratio of 200 – 400 steep increase in pore volume in lower P/P_0 indicate the presence of microporosity followed by a hysteresis loop which is indicative of messoporisity. The hysteresis loops become wider at higher P/P_0 for samples with higher R/C ratios particularly for samples with R/C ratios of 400 and 500 indicating well-developed mesoporous structures [5].This indicates the development of messoporisity and formation of larger mesopores during gelation process at higher R/C ratios.

Pore size distribution (PSD) of the RF gels is shown in Figure 2. It can be seen that the average pore size increases with increase in R/C ratio. Sample with R/C ratio of 100 shows very narrow PSD with the maxima around 2 nm. Increasing the R/C ratio to 200 increases the pore diameter above 3 nm. For the sample with R/C ratio of 500, PSD curves are even wider and pore diameter is increased to nearly 8 nm. This in mainly due to the formation of larger clusters at higher R/C ratios during the gelation process which result in inter-particle paths acting as the pores with in the structure of the final gels [13].

Table 1 Porosity parameters of aerogel samples with different R/C ratio.

Sample	R/C	S_{BET} (m^2g^{-1})	V_{total} (cm^3g^{-1})	V_{micro} (cm^3g^{-1})	V_{messo}(cm^3g^{-1})	V_{micro} %	V_{meso}%	D_{ave}(nm)
RF100	100	117	0.0714	0.0058	0.0656	8	92	2.60
RF200	200	256	0.2406	0.0011	0.2296	5	95	3.40
RF300	300	327	0.4282	0.0028	0.4254	1	99	5.20
RF400	400	313	0.5624	0.0052	0.5572	1	99	6.78
RF 500	500	322	0.6409	0.0075	0.6334	1	99	7.97

Table 1 summarizes the porosity parameters of the gel samples. As seen the mesoporosity of the samples increases with the increase in R/C ratio and this behaviour is well consistent with pore size distribution where pore size increases from 2.6 nm to 7.97 nm for samples with R/C ratios of 100 and 500 respectively.

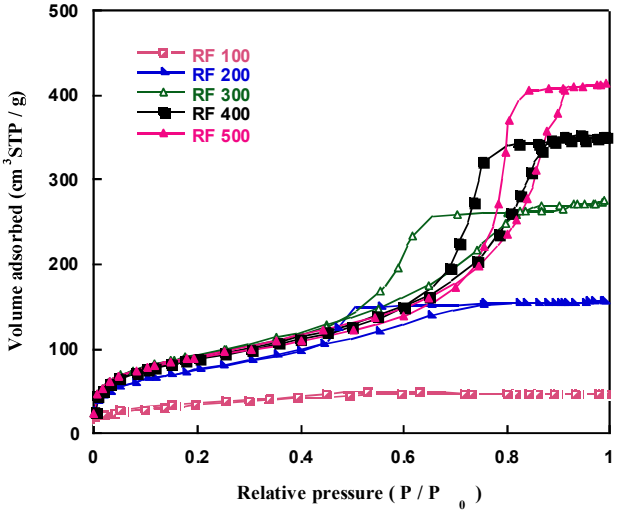

Figure 1 N_2 adsorption–desorption isotherms of R/F aerogels with different R/C ratios.

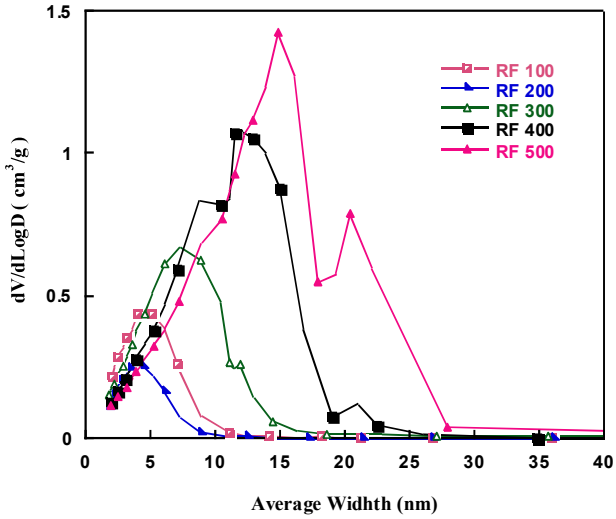

Figure 2 Pore size distribution of RF aerogels with different R/C ratios.

Figure 3 shows adsorption-desorption isotherms of the aerogel with R/C ratio of 200 used as the precursor for the preparation of the carbon aerogels and the isotherms for carbon aerogels produced at different temperatures. It can be observed that carbonization results in enormous increase in the specific surface area for all samples. A significant increase in volume adsorbed at lower $P/P_0 < 0.2$ shows the development of microporosity whereas hysteresis loops at relative pressure P/P_0 between 0.4 – 1.0 indicates the presence of messo-porosity in the samples [14]. A decrease in adsorbed volume at temperatures above 800 ºC can be the result of the collapse of the pore structure at high temperatures [15].

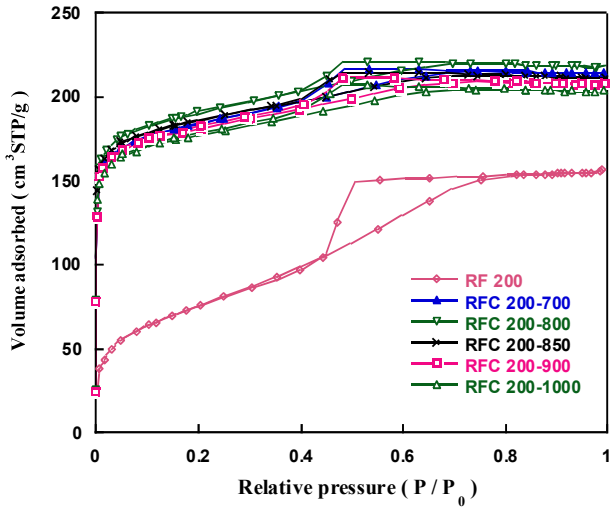

Figure 3 N_2 adsorption–desorption isotherms of carbon aerogels produced at different temperatures.

Figure 4 shows the pore size distribution curves for carbon aerogels obtained at different temperatures. The PSD curves show a bimodal trend for carbons indicating the presence of both micropores cantered around 2 nm and small mesopores cantered around 4 nm within their structure [16]. This is mainly due to the opening of close micropores during the pyrolysis process. It can be seen that due to the structural change and release of volatile matters during the carbonisation process the level of messoporisity in the resultant carbons also decreases. This means the carbonisation opens more micropores and at the same time decreases the level of messoporisity as a result structural change as a result of the release of light components of the gel at elevated temperatures.

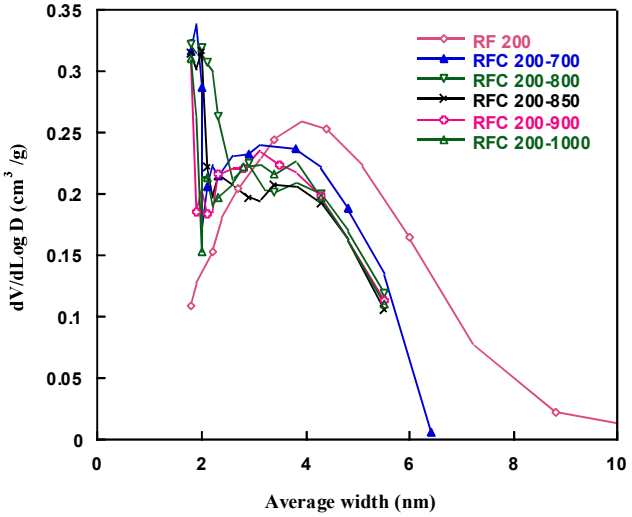

Figure 4 Pore size distribution of carbon aerogels produced at different temperatures.

Table 2 shows the porosity parameters of the RF 200 aerogel and RFC 200 carbon aerogels produced at different temperatures.

Table 2 Porosity parameters of the RF 200 aerogel and RFC 200 carbon aerogels produced at different temperatures.

Sample	S_{BET} (m^2g^{-1})	V_{total} (cm^3g^{-1})	$V_{micro\%}$	$V_{meso\%}$	D_{ave}(nm)
RF 200	256	0.2406	5	95	3.8
RFC 200- 700 ºC	616	0.3321	38	62	2.1
RFC 200- 800 ºC	638	0.3373	62	38	2.1
RFC 200- 850 ºC	617	0.3269	64	36	2.1
RFC 200- 900 ºC	604	0.3214	66	34	2.1
RFC 200-1000 ºC	586	0.3149	65	35	2.2

The specific surface area increases due to carbonization of the gel samples with highest surface area obtained at 800 ºC. However for carbons produced at temperatures above 800 ºC a gradual decrease in surface area is observed. Temperature of 800 ºC is the most effective for the development of the pore structure of the gel and increasing the carbonization temperature beyond this temperature results in the collapse of the carbon structure and decrease in the porosity. The temperature of 800 ºC is considered as the optimum temperature for the preparation of carbon aerogels with different R/C ratio.

N_2 adsorption–desorption isotherms of the carbons and activated carbons at different activation temperatures are shown in Figure 5.

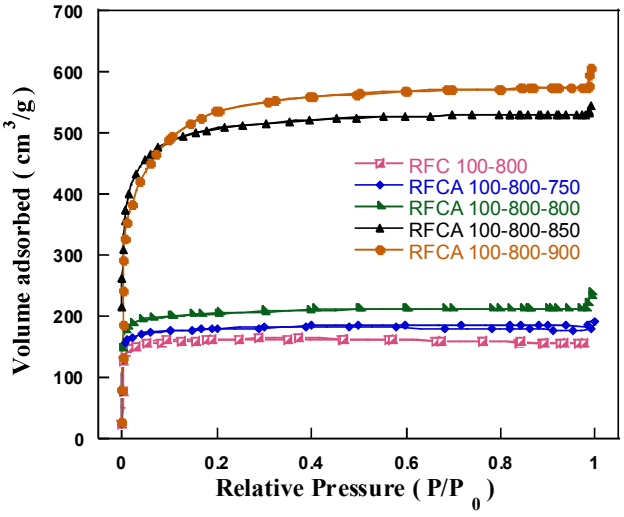

Figure 5 – N_2 adsorption–desorption isotherms of carbon / activated carbon aerogels.

The isotherms show a sharp increase in the amount of gas adsorbed at low pressures in the range of $P/P_0 < 0.01$ indicating the development of microporosity in carbon structure due to the physical activation. This is followed by a hysteresis loop in P/P_0 range 0.4-0.9 which represents the development of mesoporisity within the activated carbon samples [17]. The lower part of the hysteresis loops represent the filling of the mesopores while the upper parts represent the emptying of the mesopores [18]. With the increase in activation temperature the volume of gas adsorbed increases due to the development of porosity in the samples.

Pore size distribution (PSD) of carbon / activated carbon aerogels is represented in Figure 6 indicating all samples are predominantly microporous in nature with a pore size distribution centred around 2 nm.

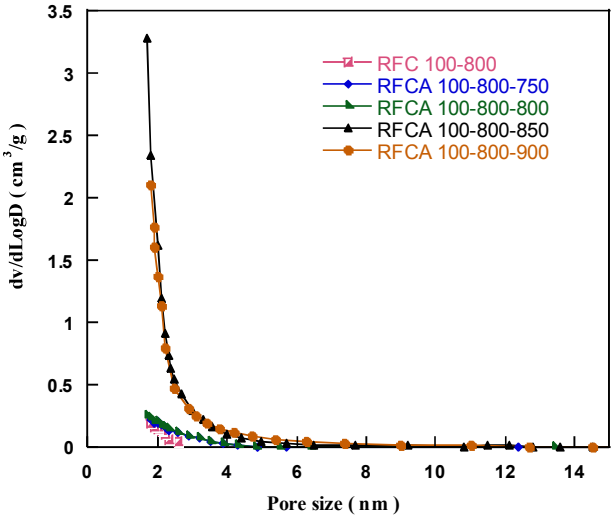

Figure 6 – Pore size distribution of carbon/activated carbon aerogels.

Table.3 shows the results of porosity analysis where significant increase in pore volume and specific surface area can be observed with the average pore size remained constant around 2nm.

Table 3 Porosity parameters of carbon/activated carbon aerogels.

Sample	S_{BET} (m^2g^{-1})	V_{total} (cm^3g^{-1})	V_{micro} %	V_{meso} %	D_{avg} (nm)
RFC 100-800	537	0.2420	90	10	1.80
RFCA 100-800-750	602	0.2981	79	21	1.99
RFCA 100-800-800	678	0.3707	72	28	2.19
RFCA 100-800-850	1687	0.8413	72	28	2.00
RFCA100-800-900	1775	0.9394	42	58	2.12

4.2 Raman spectroscopy

Figure 7 shows the Raman spectra of carbons activated at different temperatures. Activation results in well-developed porous structure however activation at very high temperatures and at higher degree of burn off, can result in decrease in the degree of graphitization [17]. Peaks shown in Figure 4 around 1340 and 1600 cm^{-1} are the characteristics peak of such carbon material [19]. The ratio I_D/I_G of the relative intensity of the D and G band is proportional to the number of defect sites in carbon, the higher the ratio is lower the degree of graphitization is [20].

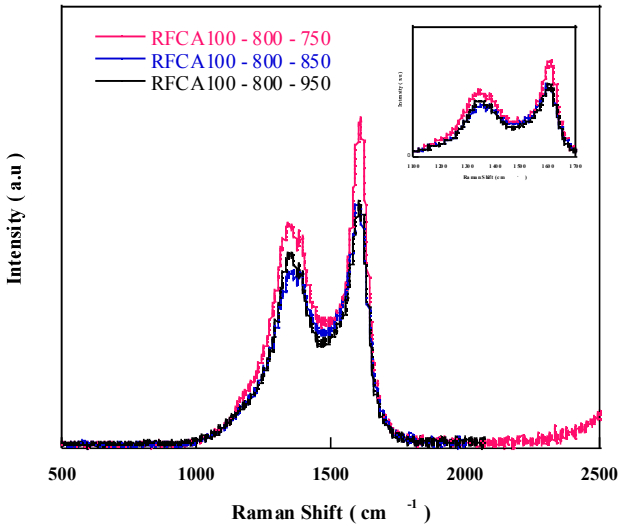

Figure 7 Raman spectra of RFCA 100-800 activated at different temperatures.

Increase in activation temperature increase the I_D/I_G values as listed in Table 4.

Table 4 Raman features of activated carbons.

Sample	Activation Temperature (^{0}C)	D Peak (cm^{-1})	G Peak (cm^{-1})	I_D / I_G
RFCA100 - 800	750	1340	1610	0.67
RFCA100 - 800	850	1340	1590	0.72
RFCA100 - 800	950	1350	1600	0.78

4.3 Contact angle measurements

The wettability of carbon /activated carbon aerogel was investigated using 6M KOH as a probing liquid. Appropriate surface modification, surface roughness, surface energy and the type of electrolyte adopted can have a significant effect on the wettability of the surface. It has been observed that nitrogen or oxygen modified surfaces interact with aqueous electrolyte with increased wettability due to the presence of nitrogen or oxygen functional groups [21]. Reduction in contact angle from 125º to 91º for carbon and activated carbons was witnessed as shown in table 5.

Table 5 contact angle measurements of carbon/activated carbon aerogels

Sample	RFC100-800	mRFC100-800
Contact angle	125º	91º

2. CONCLUSIONS

Resorcinol-formaldehyde aerogels were synthesised by sol–gel polycondensation reaction. Effect of R/C ratio, carbonization / activation temperature on physical properties such as the porous structure, degree of graphitization and wetting behaviour was assessed. Increase in R/C ratio led to increase in pore size of

aerogels whereas decrease in average pore size along with increase in specific surface area was witnessed which can be credited to the release of volatile maters and opening of closed micropores after carbonization for temperatures up to 800 °C. . Increasing the carbonization beyond 800 °C decreases the pore volume and surface area of the resultant carbons as a result of the collapse of their porous structure. Threefold increase in specific surface area of carbon aerogel samples was observed after activation whereas average pore size remained unchanged (around 2nm). Improved wetting behaviour was observed with the reduction in contact angle from 125º to 91º after activation which can be attributed to the introduction of oxygen functional groups. Samples became more amorphous in nature with the increase in activation temperature.

REFERENCES

[1] R. Pekala, "Organic aerogels from the polycondensation of resorcinol with formaldehyde," *Journal of materials science,* vol. 24, pp. 3221-3227, 1989.

[2] R. W. Pekala, "Synthetic control of molecular structure in organic aerogels," *MRS Online Proceedings Library Archive,* vol. 171, 1989.

[3] R. Pekala, C. Alviso, F. Kong, and S. Hulsey, "Aerogels derived from multifunctional organic monomers," *Journal of Non-Crystalline Solids,* vol. 145, pp. 90-98, 1992.

[4] S. A. Al-Muhtaseb and J. A. Ritter, "Preparation and properties of resorcinol–formaldehyde organic and carbon gels," *Advanced materials,* vol. 15, pp. 101-114, 2003.

[5] M. Mirzaeian and P. J. Hall, "Nano structure carbons for energy storage in lithium oxygen batteries," in *Sustainable Power Generation and Supply, 2009. SUPERGEN'09. International Conference on*, 2009, pp. 1-10.

[6] M. Mirzaeian and P. J. Hall, "Preparation of controlled porosity carbon aerogels for energy storage in rechargeable lithium oxygen batteries," *Electrochimica Acta,* vol. 54, pp. 7444-7451, 2009.

[7] E. P. Barrett, L. G. Joyner, and P. P. Halenda, "The determination of pore volume and area distributions in porous substances. I. Computations from nitrogen isotherms," *Journal of the American Chemical society,* vol. 73, pp. 373-380, 1951.

[8] F. B. Sillars, S. I. Fletcher, M. Mirzaeian, and P. J. Hall, "Effect of activated carbon xerogel pore size on the capacitance performance of ionic liquid electrolytes," *Energy & Environmental Science,* vol. 4, pp. 695-706, 2011.

[9] Q. Abbas, M. Mirzaeian, and A. A. Ogwu, "Electrochemical performance of controlled porosity resorcinol/formaldehyde based carbons as electrode materials for supercapacitor applications," *International Journal of Hydrogen Energy,* 2017.

[10] Q. Abbas, M. Mirzaeian, and A. A. Ogwu, *Improving the Functionality of Resorcinol-Formaldehyde Based Carbon Aerogels as Electrode Material for Supercapacitor Applications*, 2017.

[11] A. J. Rennie and P. J. Hall, "Nitrogen-enriched carbon electrodes in electrochemical capacitors: investigating accessible porosity using CM-SANS," *Physical Chemistry Chemical Physics,* vol. 15, pp. 16774-16778, 2013.

[12] Y. J. Lee, H. W. Park, G.-P. Kim, J. Yi, and I. K. Song, "Supercapacitive electrochemical performance of graphene-containing carbon aerogel prepared using polyethyleneimine-modified graphene oxide," *Current Applied Physics,* vol. 13, pp. 945-949, 2013.

[13] M. Mirzaeian and P. J. Hall, "The control of porosity at nano scale in resorcinol formaldehyde carbon aerogels," *Journal of materials science,* vol. 44, pp. 2705-2713, 2009.

[14] G. Ma, Q. Yang, K. Sun, H. Peng, F. Ran, X. Zhao*, et al.*, "Nitrogen-doped porous carbon derived from biomass waste for high-performance supercapacitor," *Bioresource technology,* vol. 197, pp. 137-142, 2015.

[15] E. Fiset, J.-S. Bae, T. E. Rufford, S. Bhatia, G. Q. Lu, and D. Hulicova-Jurcakova, "Effects of structural properties of silicon carbide-derived carbons on their electrochemical double-layer capacitance in aqueous and organic electrolytes," *Journal of Solid State Electrochemistry,* vol. 18, pp. 703-711, 2014.

[16] P. J. Hall, M. Mirzaeian, S. I. Fletcher, F. B. Sillars, A. J. Rennie, G. O. Shitta-Bey*, et al.*, "Energy storage in electrochemical capacitors: designing functional materials to improve performance," *Energy & Environmental Science,* vol. 3, pp. 1238-1251, 2010.

[17] M. Zhou, F. Pu, Z. Wang, and S. Guan, "Nitrogen-doped porous carbons through KOH activation with superior performance in supercapacitors," *Carbon,* vol. 68, pp. 185-194, 2014.
[18] S. J. Gregg, K. S. W. Sing, and H. Salzberg, "Adsorption surface area and porosity," *Journal of The Electrochemical Society,* vol. 114, pp. 279C-279C, 1967.
[19] M. Zhou, T. Cai, F. Pu, H. Chen, Z. Wang, H. Zhang*, et al.*, "Graphene/carbon-coated Si nanoparticle hybrids as high-performance anode materials for Li-ion batteries," *ACS applied materials & interfaces,* vol. 5, pp. 3449-3455, 2013.
[20] M. Liu, L. Gan, W. Xiong, F. Zhao, X. Fan, D. Zhu*, et al.*, "Nickel-doped activated mesoporous carbon microspheres with partially graphitic structure for supercapacitors," *Energy & Fuels,* vol. 27, pp. 1168-1173, 2013.
[21] S. L. Candelaria, B. B. Garcia, D. Liu, and G. Cao, "Nitrogen modification of highly porous carbon for improved supercapacitor performance," *Journal of Materials Chemistry,* vol. 22, pp. 9884-9889, 2012.